# Polarized small-angle light scattering from gels estimated in terms of a statistical approach

Masaru Matsuo,* Seiko Miyoshi, Mami Azuma, Yumiko Nakano, and Yuezhen Bin
*Textile and Apparel Science, Faculty of Human Life and Environment, Nara Women's University, Nara 630-8263, Japan*
(Received 30 November 2004; revised manuscript received 27 July 2005; published 21 October 2005)

To analyze polarized light scattering patterns from gels, an approach is proposed to calculate the scattered intensity. In the proposed model system, difference between polar angles of the principal axes of the *i*th and *j*th elements, which were defined with respect to the axis along the distance between two elements, was given as a correlation of the distance between the two elements. Furthermore, the azimuthal angle, which makes a projection of the *j*th principal axis onto a plane perpendicular to the principal axis of the *i*th element, was also given as a correlation of the distance between the two elements. The theoretical calculation was carried out for the scattered intensity under *Hv* and *Vv* polarization conditions. The general equations proposed for *Hv* and *Vv* scattering were based on a statistical approach for polarized light scattering system. The calculated pattern under the *Hv* polarization condition showed an X-type pattern and was in good agreement with the pattern observed from polymer gels prepared by quenching their solutions to the desired temperatures.

DOI: 10.1103/PhysRevE.72.041403 PACS number(s): 82.33.Ln, 61.25.Hq, 61.41.+e, 83.80.Kn

## I. INTRODUCTION

Light scattering from anisotropic density fluctuations was first developed by Debye and Bueche [1], and the theory was expanded to the scattering of light from a polymer film with randomly correlated orientation fluctuations of anisotropic elements by Stein and Wilson.[2] According to their paper, polarized light scattering intensities $I_{Hv}$ and $I_{Vv}$, were formulated under *Hv* and *Vv* polarization conditions, in which *Hv* and *Vv* are horizontal and vertical components, respectively, of scattered intensity observed by using a vertically ($v$) polarized incident beam. The formulated equations are as follows:

$$I_{Hv} = \frac{1}{15} K \delta^2 \int_0^\infty \mu'(r) f(r) \frac{\sinh r}{hr} r^2 dr \tag{1.1}$$

and

$$I_{Vv} = K \int_0^\infty \left\{ \langle \eta^2 \rangle_{av} \gamma(r) + \frac{4}{45} \delta^2 f(r)_{r_{ij}} \mu'(r) \right\} \frac{\sinh r}{hr} r^2 dr, \tag{1.2}$$

where

$$h = \frac{4\pi}{\lambda} \sin \frac{\theta}{2}. \tag{1.3}$$

In Eq. (1.2), $\gamma(r)$ is a correlation function for fluctuations associated with the mean-square fluctuation in average polarizability $\langle \eta^2 \rangle_{av}$. In Eqs. (1.1) and (1.2), $f(r)$ is an orientation correlation function of the principal axes between two scattering elements and $\mu'(r)$ is given by

$$\mu'(r) = 1 + \frac{\langle \Delta^2 \rangle_{av}}{\delta^2} \psi(r), \tag{1.4}$$

where $\delta$ is the average anisotropy, $\langle \Delta^2 \rangle_{av}$ is a mean-square fluctuation in average optical anisotropy, and $\psi(r)$ is the correlation function associated with the fluctuation in the magnitude of the anisotropy normalized by $\langle \Delta^2 \rangle_{av}$, which shall be discussed later in detail. If the axis ratio of the polarizability ellipsoid remains constant, $\delta$ fluctuates only because of the fluctuations in average polarizability. Under these conditions,

$$\langle \Delta^2 \rangle_{av} / \delta^2 = \langle \eta^2 \rangle_{av} / \alpha^2 \tag{1.5}$$

and $\psi(r) = \gamma(r)$, in which $\alpha$ is the average polarizability. It is well known that if there is no orientation fluctuation of the scattering elements ($f(r) = 0$), $I_{Hv}$ becomes zero, while $I_{Vv}$ becomes

$$I_{Vv} = K \langle \eta^2 \rangle_{av} \int_0^\infty \gamma(r) \frac{\sinh r}{hr} r^2 dr. \tag{1.6}$$

The above equation is similar to the equation by Debye and Bueche [1], which has been generally used to analyze the structure in terms of the profile of $\gamma(r)$ [3–6]. As for polymer gels, Pines and Prins applied to the analysis of swollen real networks within gels [3,4] by assuming that $\gamma(r)$ is described by a sum of Gaussians.

However, when solutions of crystalline polymers such as poly(vinyl alcohol) (PVA) [7] and agarose [8] solutions were quenched to the desired temperature, the phase separation was confirmed under the gelation-crystallization process. Namely, when the vertical polarized incident beam was directed to the solution under no existence of the analyzer, the logarithm of the scattered intensity increased linearly in the initial stage of the phase separation and tended to level off in the later stage. In the initial stage, the corresponding *Hv* scattering showed a circular pattern with very weak scattered

*Author to whom correspondence should be addressed. FAX: 81-742-20-3462. Electronic address: m-matsuo@cc.nara-wu.ac.jp

 

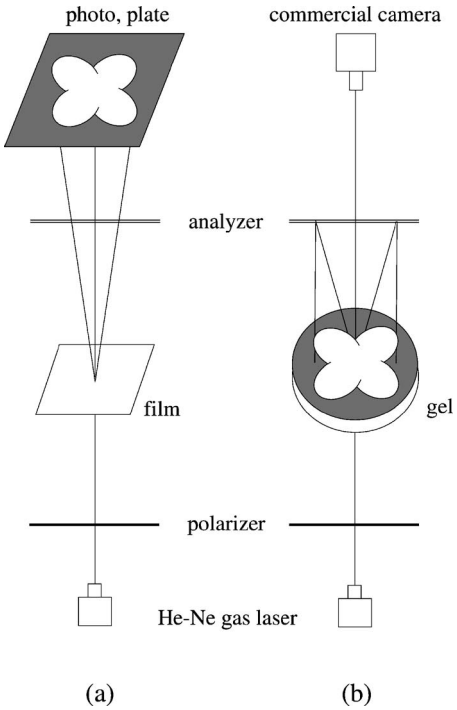


FIG. 1. Light scattering pattern from polymer gels. (a) An usual method to take the photo of the pattern. (b) The pattern reflected on the gel surface by the analyzer is taken by a commercial camera

intensity, in addition to the corresponding circular *Vv* scattering pattern with weak intensity. This indicates that the resultant polymer-rich phases are composed of scattering elements with orientation fluctuations. In such a condition, it is impossible to analyze the progression of the phase separation of the gels based on $\gamma(r)$ by using Eq. (1.6). Matsuo *et al.* [7,8] used the following equation proposed by Stein and Wilson [2] to obtain $\gamma(r)$ from such circular profiles of *Hv* and *Vv* scattering:

$$I_{V_v} - \frac{4}{3} I_{H_v} = K \langle \eta^2 \rangle_{av} \int_0^\infty \gamma(r) \frac{\sinh r}{hr} r^2 dr. \qquad (1.7)$$

In the actual analysis, the correlation distance estimating the extension of the inhomogeneities can be obtained by assuming that $\gamma(r)$ in Eqs. (1.6) and (1.7) is generally described by a sum of Gaussians [3,4,7,8].

However, progression of the phase separation of solutions provided gelation and the resultant gel became stiffer with time, indicating an increase in cross-linking points. The corresponding *Hv* pattern changed from a circular to an X type similar to the scattering from anisotropic rods, the optical axis being parallel or perpendicular to the rod axis [9,10], and the pattern becomes clearer with time. In accordance with our experimental results [7,8], the pattern under *Hv* polarization conditions was very weak and the pattern could not be observed on the photoscreen as shown in Fig. 1(a) represented as a schematic diagram, since the very weak light scattered from the gels cannot pass through the analyzer. The pattern was observed on the sample surface by the reflection from the analyzer, and then the photographs were taken by a commercial camera as shown in Fig. 1(b) [7,8]. Such weak scattered light is attributed to no existence of clear superstructure. Namely, the corresponding polarized microscopy showed a dark vision and any superstructure could not be observed, indicating that the size is not much longer than the wavelength of the He-Ne gas laser. We must emphasize that the X-type pattern from such a system is quite different from the scattering from anisotropic rods reported for the X-type scattering from poly(tetrafluorethylene) (PTFE) films [9,10]. In such a system with X-type patterns, the rods could be observed within the PTFE films clearly under polarized microscopy.

Accordingly, it is evident that the X-type pattern from such gel structures cannot be analyzed by using successful theories that have been proposed on the basis of structural models such as rods [9–11], spherulites [12,13], other tissues [14–16], and multiple light scattering [17]. Of course, the analysis by Eq. (1.7) is meaningless unless the initial stage of the phase separation provides circular-type patterns under *Hv* and *Vv* polarization conditions. Anyway, it is obvious that very weak scattered intensity from the gels under *Hv* polarization conditions has been obstructive to study the structure of anisotropic physical gels. Actually, there has been no report for polarized light scattering from anisotropic gels except our previous papers [7,8].

This paper deals with a theoretical analysis of polarized light scattering from the gels, whose *Hv* scattering can be observed as an X-type pattern by the unusual method in Fig. 1(b), in terms of a statistical approach. In this process, the density and orientation fluctuations are represented separately as each nonrandomly correlated fluctuation, as estimated by Stein and Wilson [2]. To represent the azimuthal angle dependence, a new coordinate system for the principal polarizabilities of the scattering volume elements must be adopted. This general theory can be widely applied to a structural analysis of anisotropic tissues such as gels, surfactants, and liquid crystals with orientation fluctuations between scattering elements. Of course, the theoretical calculation was provided in terms of Rayleigh-Gans theory, apart from complicated concept of Mie theory, which has been applied to isotropic spherulites [18,19].

## II. EXPERIMENT

Agarose was used as a test specimen. Agarose produced for the measurement of electrophoresis was purchased from Wako Junyaku Co. Ltd. The contents of sulfate and sulphur are less than 1.0% and 0.3%, respectively. The strength of gels is less than ca. 0.6 MPa. Distilled water ($H_2O$) was used as a solvent. The solution in a glass tube was prepared by heating the well-blended polymer/solvent mixture at 80 °C for 20 min under nitrogen. The sample was set in the sample holder of a light scattering instrument which had been controlled at 80 °C and quenched to the desired temperature. The time dependence of the scattered intensity was measured by using a vertically polarized He-Ne gas laser beam without an analyzer.

Small-angle light scattering (SALS) under *Hv* polarization conditions was observed with a 15-mV He-Ne gas laser

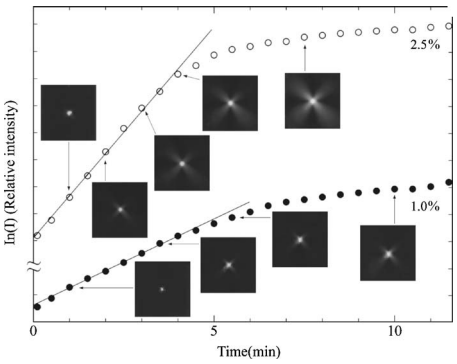


FIG. 2. Change in $\ell n(I)$ at $\theta=15°$ and $Hv$ light scattering patterns with time, which were measured for 1.0% and 2.5% agarose aqueous solutions at 30 °C.

as a light source. The light scattered from the gels could not pass through the analyzer. The reflected pattern on the gel surface was detected by a commercial camera as shown as a schematic diagram in Fig. 1(b), because the $Hv$ pattern is not due to the scattering from anisotropic superstructures whose sizes are longer than the wavelength of the He-Ne gas laser but is due to the orientation correlation of optical axes.

The x-ray measurements with Cu K$\alpha$ radiation were carried out with a 12-kW rotating-anode x-ray generator (Rigaku RDA-rA) operated at 200 mA and 40 kV. The x-ray beam was monochromatized with a curved graphite monochrometer. The time resolution of the WAXD intensity was done to study the gelation mechanism by using a curved position-sensitive proportional counter (PSPC) to estimate the change in diffraction intensity distribution as a function of the Bragg angle. The sample preparation was done by a procedure similar to the light scattering measurement.

To determine the gelation time, a test tube containing the solution in a water bath at constant temperature was titled at every 5 sec after standing 60 sec. When the meniscus deformed but the specimen did not flow under its own weight, we judged that the solution had gelled. The shortest time at which the onset of gelation occurred was defined as the gelation time.

## III. RESULTS

Figure 2 shows the change in the logarithm plots of the scattered intensity $[n(I)]$ of a He-Ne gas laser with a vertically polarized incident beam (measured without an analyzer) at a fixed scattering angle of 15° as well as the change of the corresponding $Hv$ pattern against time. The measurements were carried out for 1.0% and 2.5% agarose aqueous solutions at 30 °C. The gelation by the phase separation of the solution occurred at 180 and 120 sec for the 1.0% and 2.5% solutions, respectively. $Hv$ scattering showed an indistinct circular type, indicating the formation of a random array of quasicrystallites smaller than the wavelength of the incident beam, in the time scale showing the straight line of $\ell n(I)$ versus time $t$. This mechanism, similar to the behavior of the spinodal decomposition of amorphous blends [20], has been analyzed in terms of the initial stage of the phase separation of the solution to resolve thermodynamic unstable state by Feke and Prins [21] and Matsuo *et al.* [7,8]. With the elapsing time, the plots of $\ell n(I)$ versus $t$ deviate from the straight line and the corresponding $Hv$ scattering pattern changed from a circular type to an X type, indicating the existence of optically anisotropic rodlike textures, the optical axes being oriented parallel or perpendicular to the rod axis [9,10]. In this system, further detailed analysis provided that the spinodal temperatures of the 1.0% and 2.5% agarose aqueous solutions are 47.0 and 49.8 °C, respectively [8], which was estimated on the basis of the concept concerning the initial stage of spinodal decomposition by Cahn and Hilliard [22]. With the further lapse of time, the $Hv$ pattern became more distinct, indicating an increase in the number of rods associated with the gradual development of gelation. Nevertheless, the corresponding polarized microscopy showed a dark vision and any anisotropic rods could not be observed in the given time range. Incidentally, the $Vv$ scattering corresponding to an X-type pattern of $Hv$ scattering showed a circular-type pattern. Because of the very strong polarized intensity of an incident beam, however, the detailed shape of the scattering pattern was too indistinct to take photographs of the $Vv$ configuration.

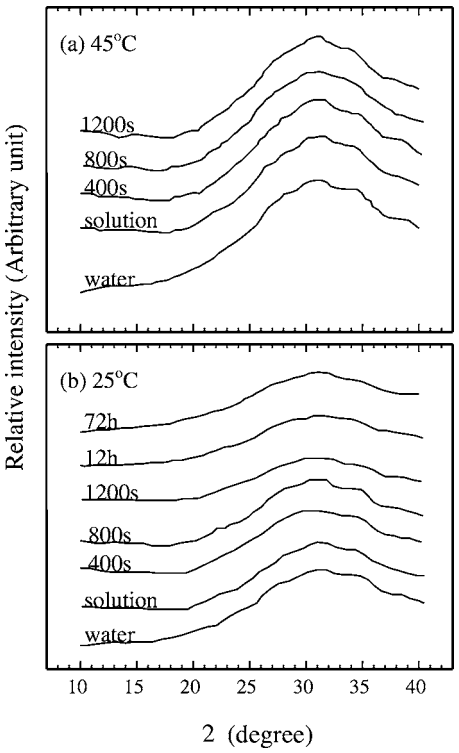


FIG. 3. Time-resolved WAXD intensity distribution as a function of twice the Bragg angle from 2.5% agarose aqueous solutions after quenching at 45 °C (upper column) or 25 °C (lower column).

A question can arise as to whether quasicrystallites with crystal lattice fluctuations were performed in the rods. To check this phenomenon, the x-ray diffraction intensity distribution was measured as a function of time, when the solution at 80 °C was quenched to 25 or 45 °C immediately. Figure 3 shows the results. The gelation times were 70 and 290 sec at 25 and 45 °C, respectively. The x-ray intensity shows a broad

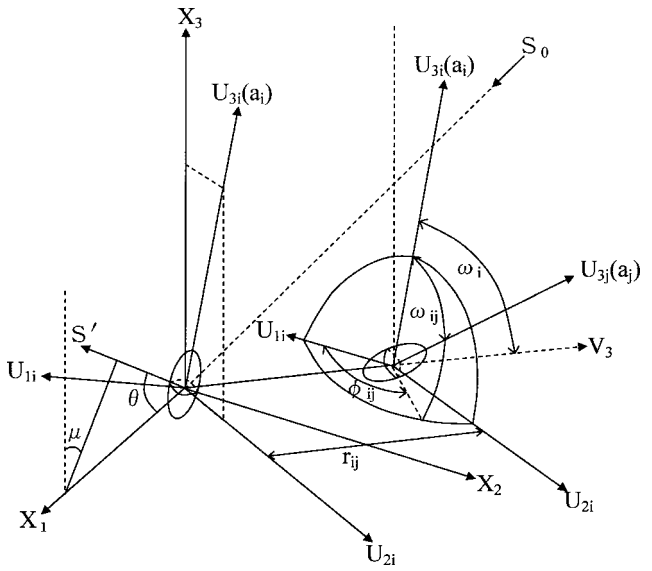


FIG. 4. Optical and coordinate system of light scattering concerning the principal polarizabilities of the scattering elements.

peak associated with the scattering due to the ordering of water molecules, and no diffraction peak from agarose crystallites is detected. The apparent observation reveals that crystallization did not occur even after 72 h. This indicates that the formation of stiff gels is independent of crystallization. This is due to the fact that (1) the molecular arrangement within the gel is too poor to derive the appearance of quasicrystallites and/or (2) cross-linking points of quasicrystallites are too few to detect by x-ray diffraction. Accordingly, it is evident that the X-type patterns are independent of scattering from anisotropic rods as the aggregation of small crystallites. Of course, as described before, the corresponding polarized microscopy showed a dark vision and any superstructure could not be observed.

Here it should be noted that Eq. (1.7) can be applied to the characteristics of gels whose scattering shows a circular pattern in the initial stage, assuring a straight line of $\ell n(I)$ versus time $t$. Namely, the values of the correlation distance estimating the extension of the inhomogeneities could be obtained by assuming $\gamma(r)$ to be the sum of Gaussian functions, which was discussed elsewhere [8]. On the other hand, we must emphasize again that the analysis of the X-type pattern under $Hv$ polarization conditions cannot be explained by the scattering from anisotropic rods and the following theoretical approach is needed.

## IV. THEORY

The scattering system is proposed as schematic diagrams in Fig. 4 to calculate $Hv$ and $Vv$ scatterings. Efforts are made to use the same notation proposed by Stein and Wilson [2] as much as possible to make clear the difference between the present model and Stein's model. As shown in Fig. 4, an incident beam denoted by a unit vector $\mathbf{s}_0$ is propagated along the $X_1$ direction and the scattered vector denoted as a unit vector $\mathbf{s}'$ is detected as a function of the scattering angle $\theta$ and azimuthal angle $\mu$ taken from the vertical direction $X_3$. The unit vectors $\mathbf{i},\mathbf{j}$, and $\mathbf{k}$ are taken along the $X_1, X_2$ and $X_3$ directions, respectively. In this system, the scattered intensity is given by

$$I = \sum_i \sum_j A_i A_j \cos\left[\frac{2\pi}{\lambda}(\mathbf{r}_{ij}\cdot\mathbf{s})\right] = \sum_i \sum_j A_i A_j \cos[k(\mathbf{r}_{ij}\cdot\mathbf{s})], \tag{4.1}$$

where $A_i$ and $A_j$ are the amplitudes of scattered intensity from the $i$th and $j$th volume scattering elements, respectively, $\lambda$ is the wavelength of light in the medium, $\mathbf{r}_{ij}=\mathbf{r}_i-\mathbf{r}_j$ is the vector between the $i$th and $j$th volume elements, and $\mathbf{s}=\mathbf{s}_0-\mathbf{s}'$. $A_i$ is proportional to the component of the dipole $\mathbf{M}_i$ induced in the $i$th scattering element by the light wave which is perpendicular to the propagation direction of the scattered ray and which is passed by a polarizer in the scattered light path—that is, if $\mathbf{O}$ is a unit vector perpendicular to $\mathbf{s}'$ and along the direction of polarization of the polarizer in the scattered beam, in which $\mathbf{O}$ corresponds to $\mathbf{k}$ and $\mathbf{j}$ for $Vv$ and $Hv$ polarizations, respectively. That is,

$$A_i = C[\mathbf{M}_i\cdot\mathbf{O}] \tag{4.2}$$

where the dipole moment induced by the effective applied field $\mathbf{E}(=E_0\mathbf{k})$ is given by

$$\mathbf{M}_i = \sum_{\ell=1}^{3} \alpha_{i\ell}(\mathbf{E}\cdot\mathbf{u}_{\ell i})\mathbf{u}_{\ell i} \text{ or } \mathbf{M}_i = \sum_{\ell=1}^{3} \alpha_{i\ell}(\mathbf{E}\cdot\mathbf{a}_{\ell i})\mathbf{a}_{\ell i}. \tag{4.3}$$

The above equation is formulated in the general anisotropic volume element with no cylindrical symmetry, and the product $\mathbf{M}_i\cdot\mathbf{O}$ for $Vv$ and $Hv$ polarization conditions is given by, for $Vv$ scattering,

$$\mathbf{M}_i\cdot\mathbf{O} = \{\alpha_{i1}(\mathbf{u}_{1i}\cdot\mathbf{k})^2 + \alpha_{i2}(\mathbf{u}_{2i}\cdot\mathbf{k})^2 + \alpha_{i3}(\mathbf{u}_{3i}\cdot\mathbf{k})^2\}E_o \tag{4.4}$$

and, for $Hv$ scattering,

$$\mathbf{M}_i\cdot\mathbf{O} = \{\alpha_{i1}(\mathbf{u}_{1i}\cdot\mathbf{k})(\mathbf{u}_{1i}\cdot\mathbf{j}) + \alpha_{i2}(\mathbf{u}_{2i}\cdot\mathbf{k})(\mathbf{u}_{2i}\cdot\mathbf{j}) + \alpha_{i3}(\mathbf{u}_{3i}\cdot\mathbf{k})(\mathbf{u}_{3i}\cdot\mathbf{j})\}E_o, \tag{4.5}$$

where $\mathbf{u}_{i1}, \mathbf{u}_{i2}$, and $\mathbf{u}_{i3}$ are unit vectors along the $U_{i1}, U_{i2}$, and $U_{i3}$ axes, respectively, for representing the three principal axes of the $i$th scattering element.

If the scattering element is rotational symmetry with respect to the $U_3$ axis, it may be described by two polarizabilities $(\alpha_\parallel)_i$ in the principal direction of the unit vector $\mathbf{u}_3$ and $(\alpha_\perp)_i$ perpendicular to this direction. That is, $\alpha_{i1}=\alpha_{i2}=(\alpha_\perp)_i$ and $\alpha_{i3}=(\alpha_\parallel)_i$.

The average polarizability of the $i$th volume element $\alpha_i$ is

$$\alpha_i = \frac{1}{3}[(\alpha_\parallel)_i + 2(\alpha_\perp)_i]. \tag{4.6}$$

When the anisotropy of the $i$th volume element is specified by $\delta_i=(\alpha_\parallel-\alpha_\perp)_i$, we have

$$(\alpha_{\parallel})_i = \alpha_i + \frac{2}{3}\delta_i, \tag{4.7}$$

$$(\alpha_{\perp})_i = \alpha_i - \frac{1}{3}\delta_i. \tag{4.8}$$

Thus the scattered intensities under *Vv* and *Hv* polarization conditions may be given as follows: for *Vv* scattering,

$$I_{Vv} = C^2 \sum_i \sum_j \left\{ \left(\alpha_i - \frac{1}{3}\delta_i\right)\left(\alpha_j - \frac{1}{3}\delta_j\right) + \left[ \delta_j \left(\alpha_i - \frac{1}{3}\delta_i\right)(\mathbf{u}_{3j}\cdot\mathbf{k})^2 + \delta_i\left(\alpha_j - \frac{1}{3}\delta_j\right)(\mathbf{u}_{3i}\cdot\mathbf{k})^2 \right] + [\delta_i\delta_j(\mathbf{u}_{3i}\cdot\mathbf{k})^2(\mathbf{u}_{3j}\cdot\mathbf{k})^2] \right\} \cos[k(\mathbf{r}_{ij}\cdot\mathbf{s})], \tag{4.9}$$

and for Hv scattering,

$$I_{Hv} = C^2 \sum_i \sum_j \delta_i\delta_j(\mathbf{u}_{3i}\cdot\mathbf{k})(\mathbf{u}_{3i}\cdot\mathbf{j})(\mathbf{u}_{3j}\cdot\mathbf{k}) \times (\mathbf{u}_{3j}\cdot\mathbf{j})\cos[k(\mathbf{r}_{ij}\cdot\mathbf{s})]. \tag{4.10}$$

In the present model system, the *i*th volume element has three kinds of fluctuations: (1) the average polarizability $\alpha_i$, (2) the anisotropy $\delta_i$, and (3) the orientation of the principal axis $U_{3i}$. To simplify the theoretical calculation, as discussed by Stein and Wilson [2], it may be assumed that the anisotropy fluctuations are not correlated with the fluctuations of average polarizability. Here we shall define

$$\eta_i = \alpha_i - \alpha, \tag{4.11}$$

where $\alpha$ is the average polarizability, and

$$\Delta_i = \delta_i - \delta, \tag{4.12}$$

where $\delta$ is the average anisotropy.

As discussed by Stein and Wilson [2], the first term of Eq. (4.9) may be given by

$$\left(\alpha_i - \frac{1}{3}\delta_i\right)\left(\alpha_j - \frac{1}{3}\delta_j\right) = \left(\alpha - \frac{1}{3}\delta\right)^2 + \left(\alpha - \frac{1}{3}\delta\right)\left[\left(\eta_i - \frac{1}{3}\Delta_i\right) + \left(\eta_j - \frac{1}{3}\Delta_j\right)\right] + \eta_i\eta_j - \frac{1}{3}[\eta_i\Delta_j + \eta_j\Delta_i] + \frac{1}{9}\Delta_i\Delta_j. \tag{4.13}$$

Of course, this must be multiplied by $\cos[k(\mathbf{r}_{ij}\cdot\mathbf{s})]$ and summed over all values of $\mathbf{r}_{ij}$. On summing, the $(\alpha - \delta/3)$ term gives zero, since this corresponds to scattering from a homogeneous medium. The second term, the products of $\eta_i$ or $\Delta_i$, and $\cos[k(\mathbf{r}_{ij}\cdot\mathbf{s})]$ average to zero, because $\mathbf{r}_{ij}$ depends on the positions of both volume elements *i* and *j*, while $\eta_i$ or $\Delta_i$ depends only the position of *i*. Consequently, if *i* is fixed and one sums over all values of *j*, the sum will be positive and negative with equal frequency.

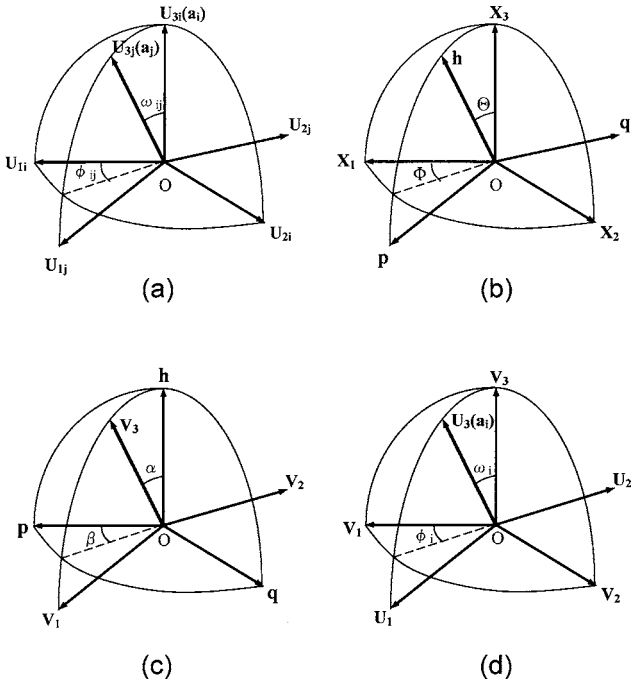


FIG. 5. Schematic diagram showing the coordinate systems for calculating light scattering. (a) Euler angles $\omega_{ij}$ and $\phi_{ij}$ of the principal axis $(U_{3j})$ of the *j*th element with respect to the Cartesian coordinates 0-$U_{1i}U_{2i}U_{3i}$ within the *i*th element. (b) Euler angles $\Theta$ and $\Phi$ specifying the orientation of the Cartesian coordinates 0-*pqh* with respect to the other Cartesian coordinates 0-$X_1X_2X_3$ fixed within a gel specimen, in which the *p* and *q* axes are perpendicular to the *h* axis. (b) Euler angles $\alpha$ and $\beta$ specifying the orientation of the Cartesian coordinates 0-$V_1V_2V_3$ with respect to the Cartesian coordinates 0-*pqh*. (d) Euler angles $\omega_i$ and $\phi_i$ specifying the orientation of the Cartesian coordinates 0-$U_1U_2U_3$ fixed within the *i*th element with respect to the Cartesian coordinates 0-$V_1V_2V_3$.

Furthermore, a correlation function for fluctuations in the average polarizability was defined by Debye and Bueche [1] as follows:

$$\gamma(r) \equiv \langle \eta_i\eta_j\rangle_r / \langle \eta^2\rangle_{av}, \tag{4.14}$$

where $\langle \eta_i\eta_j\rangle_r$ represents an average over all pairs of volume elements at constant scalar separation *r* and $\langle \eta^2\rangle_{av}$ is the mean-square fluctuations in average polarizability.

Furthermore, Stein and Wilson [2] defined a similar correlation function for fluctuations in the magnitude of the anisotropy as

$$\psi(r) = \langle \Delta_i\Delta_j\rangle_r / \langle \Delta^2\rangle_{av}. \tag{4.15}$$

As discussed in the Introduction, it is evident that $\delta$ fluctuates only because of the fluctuations in average polarizability, if the axis ratio of the polarizability ellipsoid remains constant. Under these conditions,

$$\langle \Delta^2\rangle_{av}/\delta^2 = \langle \eta^2\rangle_{av}/\alpha^2 \tag{4.16}$$

and $\psi(r) = \gamma(r)$.

To pursue the theoretical calculation based on the model system in Fig. 4, the following four Cartesian coordinates are proposed in Fig. 5.

In coordinate (a) in Fig. 5, the unit vector $\mathbf{u}_{3j}$ along the $U_{3j}$ axis is given by

$$\boldsymbol{u}_{3j} = \boldsymbol{a}_j = \cos\omega_{ij}\boldsymbol{u}_{3i} + \sin\omega_{ij}\sin\phi_{ij}\boldsymbol{u}_{2i} + \sin\omega_{ij}\cos\phi_{ij}\boldsymbol{u}_{1i}, \tag{4.17}$$

where $\omega_{ij}$ is the angle between the principal axis of the $i$th element and that of the $j$th element and depends on the length of $\mathbf{r}_{ij}$ connecting the $i$th and $j$th elements but not on the direction $\alpha$. Here $\phi_{ij}$ is the azimuthal angle of the $U_{3j}$ axis (the principal axis of the $j$th element) in the coordinate $0\text{-}U_{1i}, U_{2i}, U_{3i}$ of the $i$th element and also depends on the length of $\mathbf{r}_{ij}$ but not on the direction $\alpha$. Following Stein and Wilson [2], $\phi_{ij}$ was random around the $U_{3i}$ axis, and consequently their calculation induced independence of the azimuthal angle $\mu$ of the scattered intensity distribution [see Eqs. (1.1) and (1.2)]. Obviously, their analysis has a serious defect, since $\phi_{ij}$ must be dependent on the length of $\mathbf{r}_{ij}$. It is reasonable that $\phi_{ij}$ must be essentially zero at $\mathbf{r}_{ij}=0$, since the $i$th element coincides with the $j$th element for gel structures. Furthermore $\phi_{ij}$ is generally not random because of poor molecular chain mobility within gels. As described already, the $Hv$ scattering from the gels provided a very weak X-type pattern similar to the scattering from anisotropic rods, although polarized microscopy showed dark sight.

To give the $\mu$ dependence of the scattered intensity distribution, the following new coordinates (b), (c), and (d) in Fig. 5 are needed [23]. By using coordinate (b), the orthogonal matrices of the coordinate transformation with respect to the coordinates are given by

$$\begin{pmatrix} \mathbf{h} \\ \mathbf{q} \\ \mathbf{r} \end{pmatrix} = \begin{pmatrix} \cos\Theta & \sin\Theta\sin\Phi & \sin\Theta\cos\Phi \\ 0 & \cos\Phi & -\sin\Phi \\ -\sin\Theta & \cos\Theta\sin\Phi & \cos\Theta\cos\Phi \end{pmatrix} \begin{pmatrix} \mathbf{k} \\ \mathbf{j} \\ \mathbf{i} \end{pmatrix}, \tag{4.18}$$

where $\mathbf{h}$ is given in relation to $\cos[k(\mathbf{r}\cdot\mathbf{s})]$ as follows:

$$\mathbf{s} = (2\pi/\lambda)[(1-\cos\theta)\mathbf{i} - \sin\theta\sin\mu\mathbf{j} - \sin\theta\cos\mu\mathbf{k}]$$
$$= (4\pi/\lambda)sin\frac{\theta}{2}\mathbf{h} = h\mathbf{h}. \tag{4.19}$$

$\mathbf{h}, \mathbf{p}$, and $\mathbf{q}$ are unit vectors perpendicular to each other.

In comparison with Eq. (4.19), Eq. (4.18) can be written as follows:

$$\begin{pmatrix} \mathbf{h} \\ \mathbf{q} \\ \mathbf{r} \end{pmatrix} = \begin{pmatrix} -\cos\frac{\theta}{2}\cos\mu & -\cos\frac{\theta}{2}\sin\mu & \sin\frac{\theta}{2} \\ 0 & \sin\frac{\theta}{2}J^{-1/2} & \cos\frac{\theta}{2}\sin\mu J^{-1/2} \\ -J^{1/2} & \cos^2\frac{\theta}{2}\sin\mu\cos\mu J^{-1/2} & -\sin\frac{\theta}{2}\cos\frac{\theta}{2}\cos\mu J^{-1/2} \end{pmatrix} \begin{pmatrix} \mathbf{k} \\ \mathbf{j} \\ \mathbf{i} \end{pmatrix}, \tag{4.20}$$

where

$$J = \cos^2\frac{\theta}{2}\sin^2\mu + \sin^2\frac{\theta}{2}. \tag{4.21}$$

Here we shall define the unit vectors $\mathbf{v}_3, \mathbf{v}_2$, and $\mathbf{v}_1$ along the $V_3, V_2$, and $V_1$ axes, respectively, in which $\mathbf{v}_3$ is a unit vector of $\mathbf{r}_{ij}$ along the $V_3$ axis. Hence, from coordinate (c), we have

$$\begin{pmatrix} \mathbf{v}_3 \\ \mathbf{v}_2 \\ \mathbf{v}_1 \end{pmatrix} = \begin{pmatrix} \cos\alpha & \sin\alpha\sin\beta & \sin\alpha\cos\beta \\ 0 & \cos\beta & -\sin\beta \\ -\sin\alpha & \cos\alpha\sin\beta & \cos\alpha\cos\beta \end{pmatrix} \begin{pmatrix} \mathbf{h} \\ \mathbf{q} \\ \mathbf{p} \end{pmatrix}. \tag{4.22}$$

In the above system, the product $(\mathbf{r}_{ij}\cdot\mathbf{s})$ is given by

$$(\mathbf{r}_{ij}\cdot\mathbf{s}) = r_{ij}h(\mathbf{v}_3\cdot\mathbf{h}) = \frac{4\pi}{\lambda}\sin\frac{\theta}{2}r_{ij}\cos\alpha = hr_{ij}\cos\alpha. \tag{4.23}$$

In coordinate (d), the Euler angles $\omega_i$ and $\phi_i$ specify the orientation of the Cartesian coordinates $0\text{-}U_1U_2U_3$ fixed within the $i$th element with respect to the Cartesian coordinates $0\text{-}V_1V_2V_3$. Then we have

$$\begin{pmatrix} \mathbf{u}_{3i} \\ \mathbf{u}_{2i} \\ \mathbf{u}_{1i} \end{pmatrix} = \begin{pmatrix} \cos\omega_i & \sin\omega_i\sin\phi_i & \sin\omega_i\cos\phi_i \\ 0 & \cos\phi_i & -\sin\phi_i \\ -\sin\omega_i & \cos\omega_i\sin\phi_i & \cos\omega_i\cos\phi_i \end{pmatrix} \begin{pmatrix} \mathbf{v}_3 \\ \mathbf{v}_2 \\ \mathbf{v}_1 \end{pmatrix}. \tag{4.24}$$

$(\mathbf{M}_i\cdot\mathbf{O})$ $(\mathbf{M}_j\cdot\mathbf{O})$ for $Hv$ scattering can be obtained by using Eqs. (4.10), (4.17), and (4.19)–(4.23). However, the result is too much complicated to be written explicitly, and then the mathematical derivation is not represented.

Now, after integrating the resultant complicated equation by $\omega_1, \phi_i$, and $\beta$ with random orientation, we have

$$I_{Hv} = C^2 \int_0^{\pi} \int_0^{\infty} \mu'(r) \Bigg\{ \frac{1}{15} \left\langle \frac{3\cos^2\omega_{ij} - 1}{2} \right\rangle_{r_{ij}} + \langle 2\cos^2\phi_{ij} - 1 \rangle_{r_{ij}} \left( 1 - \left\langle \frac{3\cos^2\omega_{ij} - 1}{2} \right\rangle_{r_{ij}} \right) \Bigg[ \frac{1}{720}(5\cos^4\alpha + 30\cos^2\alpha - 11) - \frac{1}{144}\cos^2\frac{\theta}{2}(5\cos^4\alpha + 6\cos^2\alpha - 3) + \frac{1}{576}\cos^4\frac{\theta}{2}\sin^2 2\ \mu(35\cos^4\alpha - 30\cos^2\alpha + 3) \Bigg] \Bigg\} \times \cos[h r_{ij} \cos\alpha] r_{ij}^2 \sin\alpha dr_{ij} d\alpha, \quad (4.25)$$

where

$$\mu'(r) = 1 + \frac{\langle \Delta^2 \rangle_{av}}{\delta^2} \psi(r). \quad (4.26)$$

$\mu'(r)$ is equal to $\mu(r)$ defined by Stein and Wilson [2] but in the present paper $\mu$ is used as the azimuthal angle of the scattered beam as shown in Fig. 4. Hence $\mu'(r)$ is used instead of $\mu(r)$.

An orientation correlation function associated with the angle between two principal axes is defined by Stein and Wilson [2]. By omitting the dummy subscript $ij$ for $r_{ij}$., it is given by

$$f(r) = \left\langle \frac{3\cos^2\omega_{ij} - 1}{2} \right\rangle_r, \quad (4.27)$$

where the average is taken over all pairs of volume elements ($i$ and $j$) separated by a constant scalar distance $r$. $f(r)=1$ for parallel orientation ($\omega_{ij}=0°$) and 0 for random orientation ($\omega_{ij}$: random), and it varies between these limits as $r$ changes from zero to infinity. The distance over $f(r)$ remains large as a measure of the size of a region within which principal axes tend to have parallel orientation.

Furthermore, as discussed before, it is important to consider that the azimuthal angle, which the projection of the $j$th principal axis onto a plane perpendicular to the principal axis of the $i$th element makes, is also given as a correlation of the distance between the two elements. In this paper, the correlation function $g(r)$ is defined as

$$g(r) = \langle 2\cos^2\phi_{ij} - 1 \rangle_r, \quad (4.28)$$

where the average is taken over all pairs of volume elements ($i$ and $j$) separated by a constant scalar distance $r$. $g(r)=1$ for parallel orientation ($\phi_{ij}=0°$) and 0 for random orientation ($\phi_{ij}$: random), and it varies between these limits as $r$ changes from zero to infinity.

In this case, $I_{Hv}$ can be written as follows:

$$I_{Hv} = K\delta^2 \int_0^{\pi} \int_0^{\infty} \mu'(r) \Bigg\{ \frac{1}{15} f(r) + g(r)[1 - f(r)] \times \Bigg[ \frac{1}{720}(5\cos^4\alpha + 30\cos^2\alpha - 11) - \frac{1}{144}\cos^2\frac{\theta}{2}(5\cos^4\alpha + 6\cos^2\alpha - 3) + \frac{1}{576}\cos^4\frac{\theta}{2}\sin^2 2\mu(35\cos^4\alpha - 30\cos^2\alpha + 3) \Bigg] \Bigg\} \times \cos[hr\cos\alpha] r^2 \sin\alpha dr d\alpha. \quad (4.29)$$

Equation (4.29) means that $\mu'(r)$ is independent of the shape of the scattering pattern because of no $\mu$-dependence, while $g(r)$ and $f(r)$ are sensitive to the profile of the scattering pattern. If $\phi_{ij}$ is random, $g(r)$ becomes zero. In this case,

$$I_{Hv} = \frac{1}{15} K\delta^2 \int_0^{\pi} \int_0^{\infty} \mu'(r) f(r) \cos[hr\cos\alpha] r^2 \sin\alpha dr d\alpha. \quad (4.30)$$

This equation can be integrated by $\alpha$ and reduces to Eq. (1.1) derived by Debye and Bueche [1].

By using a similar method to the calculation procedure for $Hv$ scattering, the $Vv$ scattering intensity can be obtained as follows:

$$I_{Vv} = K \int_0^{\pi} \int_0^{\infty} \Bigg\{ \langle \eta^2 \rangle_{av} \gamma(r) + \frac{4}{45}\delta^2 \left\langle \frac{3\cos^2\omega_{ij} - 1}{2} \right\rangle_r \mu'(r) + \delta^2 \langle 2\cos^2\phi_{ij} - 1 \rangle_r \left[ 1 - \left\langle \frac{3\cos^2\omega_{ij} - 1}{2} \right\rangle_r \right] \times \left[ I_{V_1} + \frac{\langle \Delta^2 \rangle_{av}}{\delta^2} \psi(r) I_{V_2} + \cos 2\mu \left( I_{V_3} + \frac{\langle \Delta^2 \rangle_{av}}{\delta^2} \psi(r) I_{V_4} \right) + \cos 4\mu\mu'(r) I_{V_5} \right] \Bigg\} \cos[hr\cos\alpha] r^2 \sin\alpha dr d\alpha, \quad (4.31)$$

where

$$I_{V_1} = \frac{1}{720}(15\cos^4\alpha - 30\cos^2\alpha + 7) - \frac{1}{48}\cos^2\frac{\theta}{2}(5\cos^4\alpha - 6\cos^2\alpha + 1) + \frac{1}{384}\cos^4\frac{\theta}{2}(35\cos^4\alpha - 30\cos^2\alpha + 3), \quad (4.32)$$

$$I_{V_2} = \frac{1}{2160}(45\cos^4\alpha + 30\cos^2\alpha - 19) - \frac{1}{144}\cos^2\frac{\theta}{2}(15\cos^4\alpha - 6\cos^2\alpha - 1) + \frac{1}{384}\cos^4\frac{\theta}{2}(35\cos^4\alpha - 30\cos^2\alpha + 3), \quad (4.33)$$

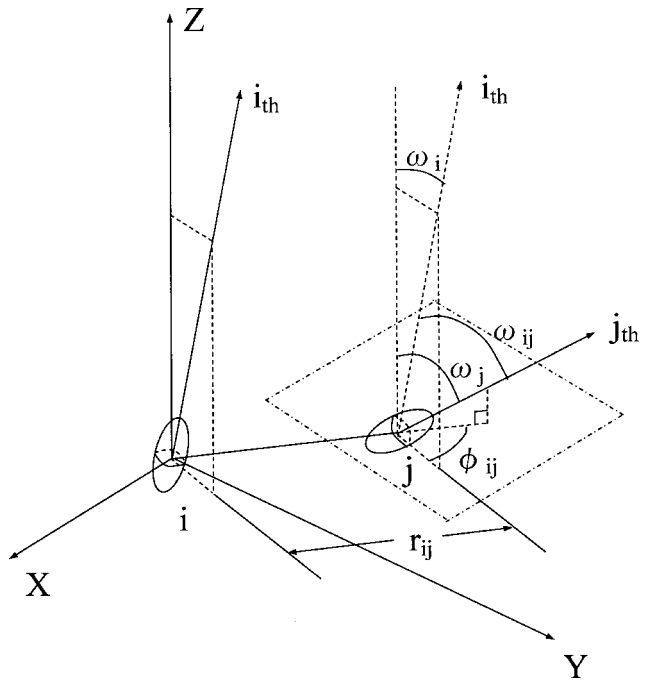


FIG. 6. The coordinate system for the principal polarizabilities of the scattering elements proposed by Stein and Wilson [2].

$$I_{V_3} = \frac{1}{48}\cos^2\frac{\theta}{2}\left(-5\cos^4\alpha 1 + 6\cos^2\alpha - 1\right) + \frac{1}{288}\cos^4\frac{\theta}{2}\left(35\cos^4\alpha - 30\cos^2\alpha + 3\right), \quad (4.34)$$

$$I_{V_4} = \frac{1}{144}\cos^2\frac{\theta}{2}\left(-15\cos^4\alpha + 6\cos^2\alpha - 1\right) + \frac{1}{288}\cos^4\frac{\theta}{2}\left(35\cos^4\alpha - 30\cos^2\alpha + 3\right), \quad (4.35)$$

$$I_{V_5} = \frac{1}{1152}\left(35\cos^4\alpha - 30\cos^2\alpha + 3\right). \quad (4.36)$$

By using Eqs. (4.27) and (4.28), Eq. (4.31) can be rewritten as

$$I_{Vv} = K\int_0^\pi \int_0^\infty \left\{ \langle \eta^2 \rangle_{av} \gamma(r) + \frac{4}{45}\delta^2 f(r)_{r_{ij}} \mu'(r) + \delta^2 g(r)[1 - f(r)]\mu'(r)\left[ I_{V_1} + \frac{\langle \Delta^2 \rangle_{av}}{\delta^2}\psi(r) I_{V_2} + \cos 2\mu\left( I_{V_3} + \frac{\langle \Delta^2 \rangle_{av}}{\delta^2}\psi(r) I_{V4}\right) + \cos 4\mu\mu'(r) I_{V_5}\right]\right\} \times \cos[hr\cos\alpha] r^2 \sin\alpha dr d\alpha. \quad (4.37)$$

If $\phi_{ij}$ is random, $g(r)$ becomes zero. In this case,

$$I_{Vv} = K\int_0^\pi \int_0^\infty \left\{ \langle \eta^2 \rangle_{av} \gamma(r) + \frac{4}{45}\delta^2 f(r)_{r_{ij}} \mu'(r)\right\} \times \cos[hr\cos\alpha] r^2 \sin\alpha dr d\alpha. \quad (4.38)$$

This equation can be integrated by $\alpha$ and reduces to Eq. (1.2) derived by Stein and Wilson [2]. Thus, Eq. (1.7) can be obtained automatically.

Here it should be noted that Eqs. (1.1) and (1.2) derived by Stein and Wilson [2] have no $\mu$ dependence. The difference between their treatment and the present one is the selection of coordinates. They adopted the coordinates shown in Fig. 6. In their model system, $\omega_i$ is related to the $X_3$ axis instead of the $V_3$ axis, which is essentially unfavorable to provide the orientation correlation function $f(r)$ in relation to the scalar distance $r$ between the two elements. Consequently, even if $\phi_{ij}$ is related to the volume elements ($i$ and $j$) separated by a constant scalar distance $r$ [see Eq. (4.28)], any $\mu$ dependence cannot be formulated on the basis of their model system in Fig. 6. When the present system shown in Fig. 4 is adopted, the mathematical treatment is extremely complicated because of complicated transformations of the coordinates in Fig. 5, and then the mathematical derivations in the present paper must be pursued by using a computer.

## V. RESULTS AND DISCUSSION

As shown in Fig. 2, the *Hv* scattering from anisotropic gels showed an X-type pattern. The numerical calculation of *Hv* scattering patterns is also favorable to avoid various selections of the parameters. Here we must emphasize again that the azimuthal angle $\phi_{ij}$ must be correlated with the distance between the two scattering elements. If not, $g(r)$ with a random orientation becomes zero. In this case, any $\mu$ dependence of the scattered intensity distribution cannot be realized as described already. Equation (4.29) can be integrated by $r$, and after that the integration for $\alpha$ must be carried out by a computer as a numerical calculation. In doing so, $f(r)$ and $g(r)$ are given as a Gaussian function as follows:

$$f(r) = \left\langle \frac{3\cos^2\omega_{ij} - 1}{2} \right\rangle_r = \exp\left(-\frac{r^2}{a^2}\right) \quad (5.1)$$

and

$$g(r) = \langle 2\cos^2\phi_{ij} - 1\rangle_r = \exp\left(-\frac{r^2}{b^2}\right). \quad (5.2)$$

Then,

$$f(r)g(r) = \exp\left\{-\left(\frac{1}{a^2} + \frac{1}{b^2}\right)\right\} = \exp\left(-\frac{r^2}{c^2}\right). \quad (5.3)$$

Of course, $f(r)$ satisfies unity at $r \to 0$ and 0 at $r \to \infty$, indicating a random correlation of the principal optical axes, and $g(r)$ also satisfies the above condition. Judging from Eq. (4.29), $f(r)$ and $g(r)$ are sensitive to the profile of the scattering pattern, while, as described already, $\mu'(r)$ is independent of the azimuthal angle. Hence $\mu'(r)$ is assumed to be a constant to simplify the analysis of the scattering patterns by

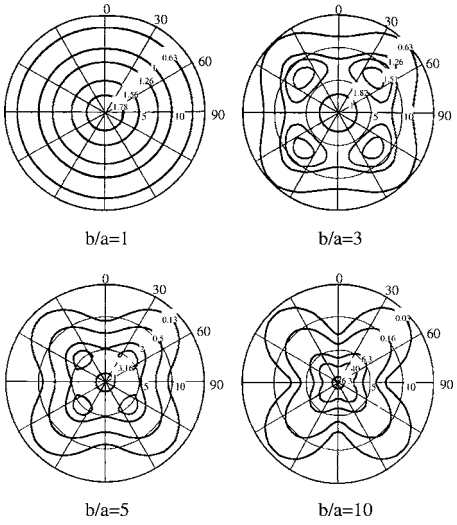


FIG. 7. *Hv* light scattering patterns calculated by Eq. (4.29) as a function of $b/a$: (a) 1, (b) 3, (c) 5, and (d) 10 at $a/\lambda=1$.

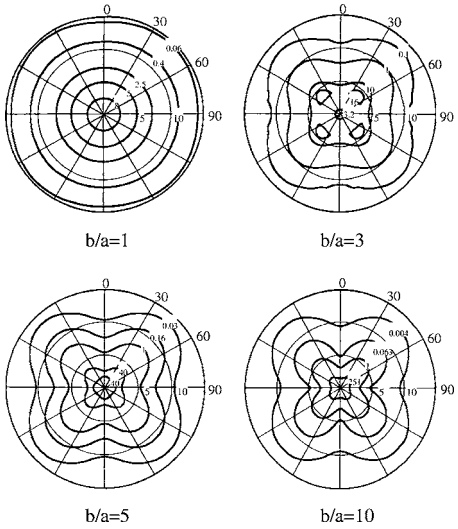


FIG. 8. *Hv* light scattering patterns calculated by Eq. (4.29) as a function of $b/a$: (a) 1, (b) 3, (c) 5, and (d) 10 at $a/\lambda=2$.

avoiding an increase in the parameters. By substituting Eqs. (5.1)–(5.3) into Eq. (4.29), we have

$$I_{H_v} = K\delta^2 \int_0^{\pi} \left\{ \frac{1}{60}\exp\left(-\frac{x^2}{4}\right) I_{H_1} + \frac{1}{5760}\exp\left(-\frac{y^2}{4}\right)\left(\frac{b^3}{a^3}\right) I_{H_2} - \frac{1}{5760}\exp\left(-\frac{z^2}{4}\right)\left(\frac{c^3}{a^3}\right) I_{H_3} + \frac{1}{4608}\sin^2 2\mu \left[ \exp\left(-\frac{y^2}{4}\right) \times \left(\frac{b^3}{a^3}\right) - \exp\left(-\frac{z^2}{4}\right)\left(\frac{c^3}{a^3}\right) \right] I_{H_4} \right\} \sin\alpha d\alpha, \tag{5.4}$$

where

$$I_{H_1} = 2 - x^2, \tag{5.5}$$

$$I_{H_2} = 11(y^3 - 2) + 5(2 - y^2)\left[ \cos^4\alpha + 6\cos^2\alpha - \cos^2\frac{\theta}{2}(5\cos^4\alpha + 6\cos^2\alpha - 3) \right], \tag{5.6}$$

$$I_{H_3} = 11(z^3 - 2) + 5(2 - z^2)\left[ \cos^4\alpha + 6\cos^2\alpha - \cos^2\frac{\theta}{2}(5\cos^4\alpha + 6\cos^2\alpha - 3) \right], \tag{5.7}$$

$$I_{H_4} = \cos^4\frac{\theta}{2}(2 - y^2)(35\cos^4\alpha - 30\cos^2\alpha + 3), \tag{5.8}$$

where

$$x = \frac{4\pi a}{\lambda}\sin\frac{\theta}{2}\cos\alpha, \tag{5.9}$$

$$y = \frac{4\pi b}{\lambda}\sin\frac{\theta}{2}\cos\alpha, \tag{5.10}$$

$$z = \frac{4\pi c}{\lambda}\sin\frac{\theta}{2}\cos\alpha, \tag{5.11}$$

Figures 7–9 show the *Hv* scattering patterns calculated at $a/\lambda=1$, 2, and 3. Furthermore, the values of parameter $b/a$ are chosen to be 1, 3, 5, and 10. The pattern is sensitive to $b/a$. With increasing $b/a$, the pattern shows considerable $\mu$ dependence to give an X type. At $b/a=1$, the pattern shows a circular type, indicating no $\mu$ dependence. This tendency is independent of the values of $a/\lambda$. This means that the pattern shows a circular type when the correlation functions of $f(r)$ and $g(r)$ are the same profile. This is an interesting phenomenon.

Comparing the calculated patterns with observed patterns in Fig. 2, the correlation of the distance for the azimuthal angle $\phi_{ij}$ [see Figs. 4 and 5(a)] becomes higher with elapsing time. Of course, the decrease in the rotational effect of $\phi_{ij}$ means that molecular chains within gel become less active

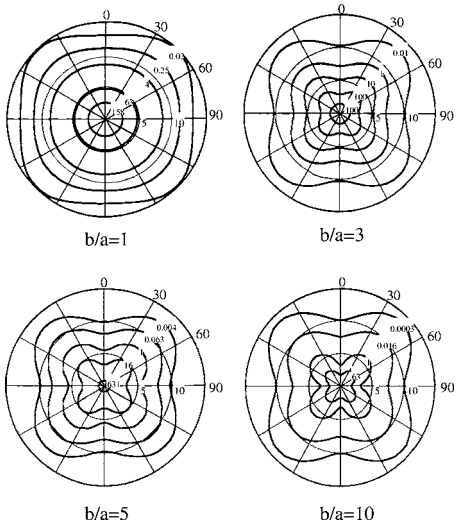


FIG. 9. *Hv* light scattering patterns calculated by Eq. (4.29) as a function of $b/a$: (a) 1, (b) 3, (c) 5, and (d) 10 at $a/\lambda=3$.

with elapsing time, since the gel becomes stiffer with increasing junction points. Certainly, no existence of anisotropic rods within the gel was confirmed under polarized microscopy, when the corresponding pattern showed an X type. A series of calculations indicates that the X-type patterns under *Hv* polarization conditions, which have been observed for polymer gels prepared by quenching solutions to desired temperature, is attributed to the high correlations between the scattering elements but is independent of the existence of the anisotropic rods. The change from a circular to an X-type pattern with elapsing time reflects the formation process of gel structure in polymer-rich phases appearing by phase separation of the agarose solution when quenching from 80 to 30 °C. Incidentally, the theory of the present paper can be applied to any anisotropic systems with orientation fluctuations between scattering elements.

## VI. CONCLUSION

*Hv* light scattering patterns were observed under the gelation process when agarose solution was quenched to a desired temperature. The *Hv* scattering showed an indistinct circular-type pattern in the initial stage and the pattern changed to an X-type pattern with elapsing time. The scattered intensity was very weak, and any anisotropic rods within the gel could not be observed under polarized microscopy. To analyze such an X-type pattern, an approach was proposed to calculate the polarized scattered intensity under *Hv* and *Vv* polarization conditions. In the proposed model system, two correlation functions concerning correlated orientation fluctuations and correlated rotational fluctuations were introduced. As a correlated orientation fluctuation, the difference between polar angles of the principal axes of *i*th and *j*th elements defined with respect to the axis along the distance between the two elements was given as a correlation of the distance between the two elements. As a correlated rotational fluctuation, the azimuthal angle, which the projection of the *j*th principal axis onto a plane perpendicular to the principal axis of the *i*th element makes, was also given as the distance between the two elements. The proposed equations for *Hv* and *Vv* scattering conditions were given as a function of the polar angle and azimuthal angle. Such an analysis is based on a general concept such as a statistical approach. In the absence of the correlation of the distance for the azimuthal angle, the reduced equations were equivalent to the equations proposed by Stein and Wilson [2]. The *Hv* scattering patterns formulated with the above two correlations showed an X-type pattern and were in good agreement with the patterns observed from polymer gels prepared by quenching their solutions to the desired temperatures. This indicated that molecular chains within the gel become less active with elapsing time, since the gel becomes stiffer with increasing junction points.

[1] P. Debye and A. Bueche, J. Appl. Phys. **20**, 518 (1949).
[2] R. S. Stein and P. R. Wilson, J. Appl. Phys. **33**, 1914 (1962).
[3] E. Pines and W. Prins, J. Polym. Sci., Part B: Polym. Lett. **10**, 719 (1972).
[4] E. Pines and W. Prins, Macromolecules **6**, 888 (1973).
[5] K. L. Wun and W. Prins, J. Polym. Sci., Polym. Phys. Ed. **12**, 533 (1974).
[6] M. Matsuo, Y. Sakai, E. Maeda, C. Hara, M. Iida, and R. S. T. Manley, J. Phys. Chem. **98**, 10988 (1994).
[7] M. Matsuo, M. Kawase, Y. Sugiura, S. Takematsu, and C. Hara, Macromolecules **26**, 4461 (1993).
[8] M. Matsuo, T. Tanaka, and L. Ma, Polymer **43**, 5299 (2002).
[9] M. Rhodes and R. S. Stein, J. Polym. Sci., Part A-2 **7**, 1539 (1969).
[10] Y. Murakami, N. Hayashi, T. Hashimoto, and H. Kawai, Polym. J. (Singapore) **4**, 452 (1973).
[11] G. Petekidis, D. Vlassopoulos, G. Fytas, R. Rulkens, and G. Wegner, Macromolecules **31**, 6129 (1998).
[12] R. S. Stein and M. B. Rhodes, J. Appl. Phys. **31**, 1873 (1960).
[13] S. Clough, J. J. van Aartsen, and R. S. Stein, J. Appl. Phys. **36**, 3072 (1965).
[14] A. Galeski and M. Kryszewski, J. Polym. Sci., Polym. Phys. Ed. **12**, 455 (1974).
[15] F. Greco, Macromolecules **22**, 4622 (1989).
[16] M. C. Newstein, B. A. Garetz, H. J. Dai, and N. P. Balsara, Macromolecules **28**, 4587 (1995).
[17] G. Fytas, D. Vlassopoulos, G. Meier, A. Likhtman, and A. N. Semenov, Phys. Rev. Lett. **76**, 3586 (1996).
[18] G. H. Meeten and P. Havard, J. Polym. Sci., Part B: Polym. Phys. **27**, 2023 (1989).
[19] G. H. Meeten and P. Havard, J. Polym. Sci., Part B: Polym. Phys. **27**, 2037 (1989).
[20] T. Nishi, T. T. Wang, and H. Kwei, Macromolecules **8**, 227 (1975).
[21] G. T. Feke and W. Prins, Macromolecules **8**, 527 (1975).
[22] J. W. Cahn and J. E. Hilliard, J. Chem. Phys. **29**, 258 (1958).
[23] M. Matsuo and K. Ihara, J. Polym. Sci., Polym. Phys. Ed. **20**, 1 (1982).